International Journal on Engineering Technology (InJET)

www.kec.edu.np/journal
Volume 1, issue no. 1, Nov 2023, Page 139-152
Received Date: June 29, 2023
Accepted Date: Nov 2, 2023
ISSN: 3021-940X (print)

Implementation of Indirect Field Oriented Control Using Space Vector Pulse Width Modulation for the Control of Induction Motor

Sabin Kasula[1 *], Bibek Shrestha[2], Karan Katwal[3], Roshan Dahal[4]

[1]*Department of Electronics and Computer Engineering, Kantipur Engineering College, Dhapakhel, Lalitpur, Nepal, sabinkasula32@gmail.com*
[2]*Department of Electrical, Cloud Himalaya Pvt. Ltd, Thapathali, Kathmandu, Nepal, bibekshrestha740@gmail.com*
[3]*Department of Electrical, Codedrops Pvt. Ltd, Kathmandu, Nepal, kkatwal40@gmail.com*
[4]*Huawei Technologies Nepal Co. Pvt. Ltd, Kathmandu, Nepal, roshandahal0525@gmail.com*

Abstract

For the efficient speed control of three phase Induction motor, the Vector control or Field oriented control (FOC) technique is used for the Voltage source inverter. In implementing FOC the angular position of the rotor flux vector is to be determined. There are two methods (direct and indirect) of vector control for the evaluation of rotor angle. In an Indirect field-oriented control (IFOC) method rotor angle is estimated from slip frequency and rotor frequency without using a sensor (sensors are used in direct FOC) which are achieved in a synchronously rotating frame. IFOC produces high performance in induction motor drives by decoupling rotor flux and torque, so it can be separately controlled by stator direct-axis current and quadrature-axis current respectively, like in a DC motor. The rotor flux orientation method is used for incorporating PI control system using the Space Vector Pulse Width Modulation (SVPWM) technique. The Induction motor drive control generally involves three different PI controllers for torque, speed, and flux respectively. Through the simulation result, varying the load torque, and reference speed is achieved within a few milliseconds, and the behavior of the separately excited DC motor is observed.

Keywords: Induction motor, Indirect field-oriented control, SVPWM, PI-controller, Decoupling

1. Introduction

Advanced control of electrical machines requires independent control of magnetic flux and torque. For that reason, the DC machine played an important role in the early days of high-performance electrical drive systems, since the magnetic flux and torque are easily controlled by the stator and rotor current, respectively. The development of field-oriented control marked a major development in electrical drives since it permits high-performance control of the robust induction machine. The working of the induction motor as the DC motor to obtain high-performing torque and speed is achieved through the decoupling method of the current components in terms of the torque and rotor flux. The selection of the induction motor is based on the demerits of the DC motor characteristics such as being less economical, and more energy-conserving. The volt/Hertz control method controls the voltage and frequency to generate the control which makes the slow transient response and does not give the desired outcomes. Other control methods like DTC and DFOC that use the application of the sensing device to sense the speed are slower compared to the IFOC which controls the phase and magnitude of the current and flux (Kumar, et al., 2007), (Hiware & Chaudhari, 2011).
SVPWM controls the output voltage of the inverter to the motor with fewer harmonics distortion, effective DC bus utilization, wide linear modulation range, and less switching time of the inverter (Tiwa & Shashank, 2017).

**Corresponding Author*

2. Literature Review

Independent control of magnetic flux and torque is necessary for advanced electrical machine control. Considering the magnetic flux and torque can be readily adjusted by the stator and rotor currents, respectively, the DC machine was crucial in the early days for high-performance electric drive systems. The introduction of Field Oriented Control is a major transformation in the field of electrical drives since with this type of control the robust Induction machine can be controlled with a high performance.
Oscillations are generated on the torque produced by the scalar control of the induction motor. However, DTC being simple allows better control of torque in transient operating conditions as well as steady state. The control of torque and flux is difficult at low speed, as it has a high current and torque ripple compared to FOC. The flux estimator is used by terminal current and voltage to obtain the rotor angle in direct FOC. The necessity of a sensor for estimating flux is difficult and costlier. The speed feedback signal of the motor calculates the rotor position in indirect FOC. The improvisation of direct FOC by eliminating the sensors, torque response, drift problems, and cost factor is done in indirect FOC. Furthermore, indirect FOC has a better dynamic performance at low speed and frequencies (BT, 2017).

2.1 *SPVWM*

Space vector PWM refers to a special switching scheme of the six power semiconductor switches of a three-phase power converter. The application of this technique has been widely used for the speed control of the induction motor and Synchronous motors. The processing of all three phases is considered as one, unlike the sinusoidal PWM method. The pulse generated is used for controlling the switches of the inverters that give the modulated outcomes to control the motor at the desired torque and speed. SVPWM methods produce the required current and voltage such that the outcomes show fewer harmonics distortion. The constant switching and the adjustment of the frequency are possible though this process is complicated while integrating into the system (Mishra, et al., 2014).

2.1.1 *Principle of SVPWM*

The typical voltage source inverter consisting of six switches is controlled to generate the pulse and output voltage and current. The on and off states of these switches determine the output voltage. The state of the upper switches and the lower ones are opposite and the condition of the upper transistor can be easily determined for the control. The eight possible combinations of these switches produce the eight-inverter voltage vector. To implement the SVPWM techniques, first, the voltage reference equation in three phase is transformed to the stationary d-q phase, d as the direct axis, and q as the quadrature axis (Jung & Jin-Woo, 2005). The relation between these two reference frames is given by the equation 1:

$$f_{dq0} = K_s f_{abc} \tag{1}$$

The projection of the three phases $[a, b, c]$ on to orthogonal reference frame to the d-q plane is possible through the transformation using the above equation. The six non-zero vectors as seen in Figure 1 transform the hexagonal axes into the space vector that provides the reference voltage. The reference voltage is thus obtained in the desired plane of the d-q through the transformation. To generate the output voltage of the inverter one can consider the period T to be in same as a reference voltage (Jung & Jin-Woo, 2005).

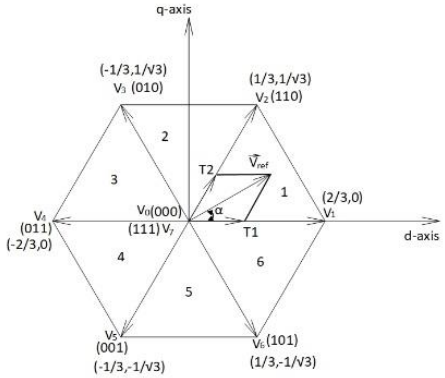

Figure 1. Basic switching vectors and sectors (Jung & Jin-Woo, 2005)

The steps for implementing the space vector pulse width modulation techniques include determining V_d, V_q , V_{ref} and angle (α), determining a time duration T_1, T_2 , T_0 and determining the switching time of each transistor (S_1 to S_6).

Step 1: Determining V_d, V_q , V_{ref} angle (α)

The determination of the position of the reference voltage in sectors gives the switching times and sequence. The location of the reference voltage is straightforward and corresponds to the eight switches. The six sectors are divided from 360 in every 60 degrees. The angle of the reference vector can be used to determine the sector depending on the reference voltages $V_\alpha$and V_β as shown in Table 1.

$$\begin{bmatrix} V_d \\ V_q \end{bmatrix} = \frac{2}{3}\begin{bmatrix} 1 & -\frac{1}{2} & -\frac{1}{2} \\ 0 & \frac{\sqrt{3}}{2} & -\frac{\sqrt{3}}{2} \end{bmatrix}\begin{bmatrix} V_{an} \\ V_{bn} \\ V_{cn} \end{bmatrix} \tag{2}$$

$$|\overline{V_{ref}}| = \sqrt{V_d^2 + V_q^2} \tag{3}$$

$$\alpha = \tan^{-1}\left(\frac{V_q}{V_d}\right) = \omega t, = 2\pi f t \tag{4}$$

where, f = fundamental frequency

Table 1. Sector Definition (Sirisha, n.d.)

Sector	Degrees
1	$0 < \theta < 60^0$
2	$60^0 < \theta < 120^0$
3	$120^0 < \theta < 180^0$
4	$180^0 < \theta < 240^0$
5	$240^0 < \theta < 300^0$
6	$300^0 < \theta < 360^0$

Step 2: Determination of time duration T_1, T_2 *and* T_0

The switching time duration at any six sectors is determined through the generalized formula of T_1, T_2 *and* T_0 as given below:

$$T_1 = \frac{\sqrt{3}.T_Z.|V_{ref}|}{V_{dc}} \sin\left(\frac{n}{3}\pi - \alpha\right) \quad (5)$$

$$T_2 = \frac{\sqrt{3}.T_Z.|V_{ref}|}{V_{dc}} \left(\sin\left(\alpha - \frac{n-1}{3}\pi\right)\right) \quad (6)$$

$$T_0 = T_z - T_1 - T_2 \quad (7)$$

where n=1 through 6 (i.e., Sector 1 to 6) [$0 \leq \alpha \leq 60^0$]

Step 3: Determining the switching time of each transistor

For the minimization of the losses from the switches, only two active vectors and two non-zero vectors are applied. Each switching period is considered to be starting from the zero vectors and ends with another zero vector to meet the required condition. (Jung & Jin-Woo, 2005)

The summarized upper and lower switch times are tabulated in Table 2:

Table 2. Switching Time Calculation at Each Sector (Jung & Jin-Woo, 2005).

Sector	Upper Switches (S_1, S_3, S_5)	Lower Switches (S_4, S_6, S_2)
1	$S1 = T_1 + T_2 + T_0/2$	$S_4 = T_0/2$
	$S_3 = T_2 + T_0/2$	$S_6 = T_1 + T_0/2$
	$S_5 = T_0/2$	$S_2 = T_1 + T_2 + T_0/2$
2	$S_1 = T_1 + T_0/2$	$S_4 = T_2 + T_0/2$
	$S_3 = T_1 + T_2 + T_0/2$	$S_6 = T_0/2$
	$S_5 = T_0/2$	$S_2 = T_1 + T_2 + T_0/2$
3	$S_1 = T_0/2$	$S_4 = T_1 + T_2 + T_0/2$
	$S_3 = T_1 + T_2 + T_0/2$	$S_6 = T_0/2$
	$S_5 = T_2 + T_0/2$	$S_2 = T_1 + T_0/2$
4	$S_1 = T_0/2$	$S_4 = T_1 + T_2 + T_0/2$
	$S_3 = T_1 + T_0/2$	$S_6 = T_2 + T_0/2$
	$S_5 = T_1 + T_2 + T_0/2$	$S_2 = T_0/2$
5	$S_1 = T_2 + T_0/2$	$S_4 = T_1 + T_0/2$
	$S_3 = T_0/2$	$S_6 = T_1 + T_2 + T_0/2$
	$S_5 = T_1 + T_2 + T_0/2$	$S_2 = T_0/2$
6	$S_1 = T_1 + T_2 + T_0/2$	$S_4 = T_0/2$
	$S_3 = T_0/2$	$S_6 = T_1 + T_2 + T_0/2$
	$S_5 = T_1 + T_0/2$	$S_2 = T_2 + T_0/2$

2.2 *Vector Control or Field-Oriented Control*

Although scalar control is very easy to use, it has a slow response due to the inherent coupling effect (both torque and flux are functions of voltage or current and frequency).
Vector or field-oriented control can be used to overcome the stated issues. A renaissance in the high-performance control of AC drives was sparked by the introduction of vector control and brought the revelation that an induction motor may be controlled like a separately stimulated DC motor. Vector control is suitable for both induction and synchronous motor drives due to its DC machine-like performance. Without a doubt,vector control and the associated feedback signal processing, particularly for modern sensorless vector control, are complex and the use of powerful microcomputers or DSP is compulsory (Bose, 2002).

2.3 Basic principle of vector control

An induction motor can be operated as a separately excited DC motor with vector control. The developed torque in a DC machine is given in equation 8,

$$T_e = K_t' I_a I_f \quad (8)$$

where, I_a is the armature current and I_f is the field current.

DC machine is built in such a way that the field flux linkage ψ_f produced by I_f is perpendicular to the armature flux linkage ψ_a produced by I_a. These flux vectors that are stationary in space are orthogonal or decoupled in nature. Hence, a DC motor has a fast transient response. However, due to the inherent coupling problems of induction motors, such a quick response is not possible. An induction motor, on the other hand, can display the DC machine characteristic if it is controlled in a synchronously rotating frame ($d_d - q_q$), where the sinusoidal machine variables appear as dc quantities in the steady state (M. H. Rashid, 2010).

The torque developed in an induction motor is given in Equation 9,

$$T_e = K_t\widehat{\psi_r}i_{qs} = K_t' i_{qs} i_{ds} \tag{9}$$

where, $\widehat{\psi_r}$ is the absolute peak value of the sinusoidal space flux linkage vector;
i_{ds} is the field component, i_{qs} is the torque component.

Under all operational circumstances, i_{ds}^* is orientated (or aligned) in the direction of rotor flux, and i_{qs}^* must be perpendicular to it. The space vectors rotate synchronously at an electrical frequency $\omega_e = \omega$. Thus, the vector control must ensure the correct orientation of the space vectors as well as generate the control input signals (M. H. Rashid, 2010).

2.4 *Direct and quadrature axis transformation*

The vector control technique uses the dynamic equivalent circuit of the Induction motor. In an induction motor, there are at least three fluxes (rotor, air gap, and stator) and three currents or mmfs (in the stator, rotor, and magnetizing). For fast dynamic response, the interaction between current, fluxes, and speed must be considered while developing the motor's dynamic model and determining effective control techniques. All fluxes rotate at synchronous speed. The three-phase currents generate mmfs (stator and rotor), which also rotate at synchronous speed. Any three-phase sinusoidal set of quantities in the stator can be transformed into an orthogonal reference frame. The orthogonal set of reference that rotates at the synchronous speed ω is referred to as d–q–0 axes.
The three-phase rotor variables are transformed to synchronously rotating. The difference $\omega - \omega_r$ is the relative speed between the synchronously rotating reference frame and the frame attached to the rotor. This difference is slip frequency ω_{sl}, which is the frequency of the rotor variables (M. H. Rashid, 2010). By applying these transformations, voltage equations of the motor in the synchronously rotating frame are reduced to,

$$\begin{bmatrix} v_{qs} \\ v_{ds} \\ v_{qr} \\ v_{dr} \end{bmatrix} = \begin{bmatrix} R_s + DL_s & \omega L_s & DL_m & \omega L_m \\ -\omega L_s & R_s + DL_s & -\omega L_m & DL_m \\ DL_m & (\omega - \omega_r)L_m & R_r + DL_r & (\omega - \omega_r)L_r \\ -(\omega - \omega_r)L_m & DL_m & -(\omega - \omega_r)L_r & R_r + DL_r \end{bmatrix} \begin{bmatrix} i_{qs} \\ i_{ds} \\ i_{qr} \\ i_{dr} \end{bmatrix} \tag{10}$$

where ω is the speed of the reference frame (or synchronous speed), ω_r rotor speed and subscripts l and m stand for leakage and magnetizing, respectively, and D represents the differential operator d/dt.

The motor slip frequency ω_{sl} is used in the indirect method to compute the desired flux vector. T_d is the desired motor torque, ψ_r is the rotor flux linkage, T_r is the rotor time constant, and L_m is the mutual inductance. Unless the flux is measured directly, the amount of decoupling is determined by the motor parameters (M. H. Rashid, 2010).

The torque developed by the motor is given in Equation 11,

$$T_d = \frac{3p}{2} \frac{[\psi_{ds} i_{qs} - \psi_{qs} i_{ds}]}{2} \tag{11}$$

To eliminate transients in the rotor flux and the coupling between the two axes, the following conditions must be satisfied i.e., $\psi_{qr} = 0$.

$$T_d = \frac{3p}{2\times2}\frac{L_m^2}{L_r} i_{ds} i_{qs} = K_m i_{ds} i_{qs} \quad (12)$$

where, $K_m = 3pL_m^2/4L_r$ (M. H. Rashid, 2010).

2.5 Indirect (or feedforward) vector control

The indirect vector control approach is very similar to direct vector control, with the exception that the cosine and sine unit vector signals (cos θ_e and sin θ_e) are produced in a feedforward way. A phasor diagram is used to demonstrate the fundamental idea of indirect vector control as shown in Figure 2. The $d_s - q_s$ axes are fixed on the stator, while the $d_r - q_r$ axes, which are fixed on the rotor, are moving at the speed ω_r as shown. The positive slip angle θ_{sl}, which corresponds to the slip frequency ω_{sl}, causes the synchronously rotating axes $d_e - q_e$ to rotate in front of the $d_r - q_r$ axes. The rotor pole is pointed at the d_e axis and $\omega_e = \omega_r + \omega_{sl}$.
The rotor pole position is not fixed but rather shifts about the rotor at the frequency ω_{sl} . For separate control or decoupling control, the torque component of the current i_{qs} should be on the q_e axis and the flux component of the stator current i_{ds} should be aligned on the d_e axis as shown in Figure 2 (M. H. Rashid, 2010).

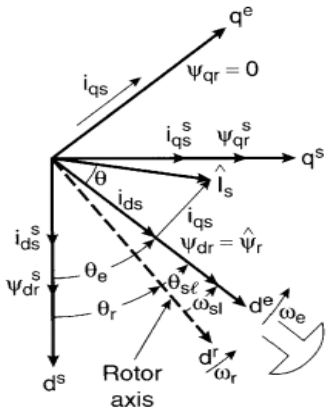

Figure 2. Phasor diagram explaining indirect vector control (Bose, 2002)

For decoupling control, it is desirable that $\psi_{qr} = 0$, i.e. $\frac{d\psi_{qr}}{dt} = 0$ So that the total rotor flux ψ_r is directed at the d_e-axis.

$$\omega_{sl} = \frac{L_m R_r}{\widehat{\psi_r}\ L_r} i_{qs} \quad (13)$$

If rotor flux $\widehat{\psi_r}$ = constant,

$$\widehat{\psi_r} = L_m i_{ds} \quad (14)$$

The rotor flux is directly proportional to the stator current i_{ds} in a steady state. The block design for the implementation of indirect field-oriented control (IFOC) can be seen in Figure 3. For the desired rotor flux ψ_r, the flux component of the current i^*_{ds} is determined and is maintained constant (M. H. Rashid, 2010).

The angular speed error $(\omega_{ref} - \omega_r)\ to\ i^*_{qs}$ is,

$$i^*_{qs} = \frac{\psi_r L_r}{L_m R_r}\ (\omega_{ref} - \omega_r) \quad (15)$$

Here, the torque component of the current i^*_{qs} is generated from the speed control loop. The slip frequency ω^*_{sl} is

generated from i^*_{qs} in a feed-forward manner. The expression of slip gain K_{sl} is given in equation 16,

$$K_{sl} = \frac{\omega^*_{sl}}{i^*_{qs}} = \frac{Lm}{\psi_r} * \frac{Rr}{L_r} = \frac{Rr}{L_r} * \frac{1}{i^*_{ds}} \quad (16)$$

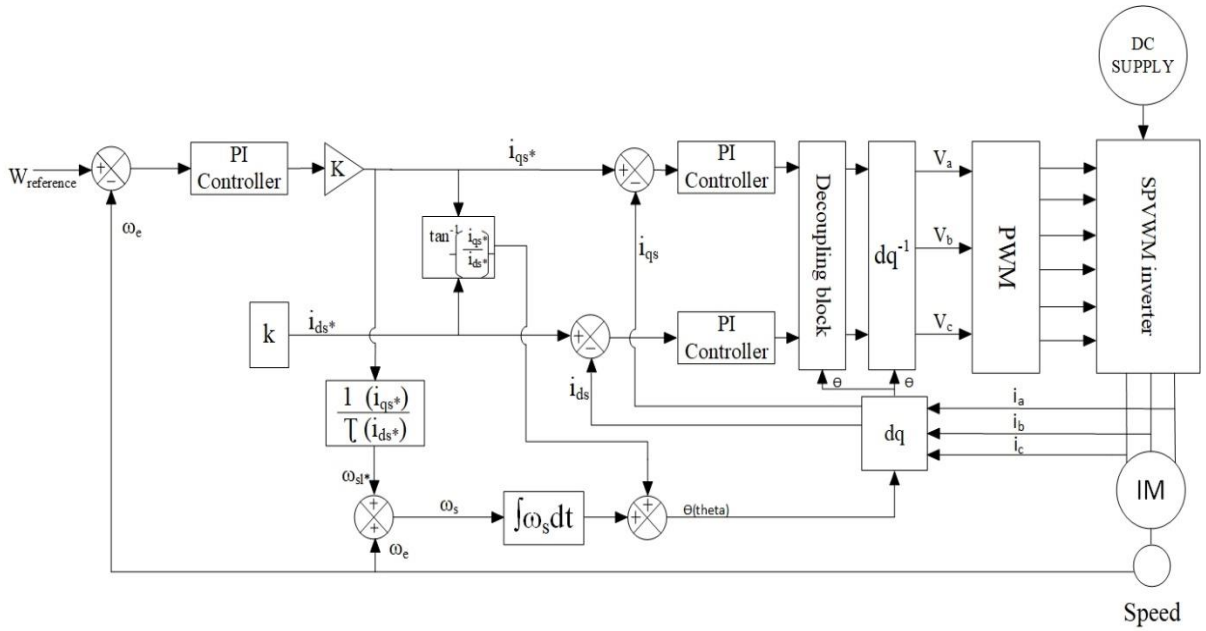

Figure 3. Indirect rotor flux-oriented control scheme.

To determine the stator frequency ω, the slip speed ω^*_{sl} is added to the rotor speed ω_r. This frequency is integrated into time to get the necessary angle θ_s of the stator mmf relative to the rotor flux vector. By using this angle, the stator currents (i_{ds} and i_{qs}) are transformed into the d_q reference frame and the unit vector signals ($\cos\theta_s$ and $\sin\theta_s$) are generated. The reference values of the i_q and i_d currents are controlled by two separate current controllers. To get switching signals for the inverter via PWM, the adjusted i_q and i_d errors are then inverse transformed into the stator a-b-c reference frames. This technique uses a feed-forward scheme to produce ω^*_{sl} from i^*_{ds}, i^*_{qs} and T_r. For some operating conditions, the rotor time constant T_r might not be constant. As a result, the slip speed ω_{sl}, which directly impacts the generated torque and the rotor flux vector position, may differ greatly. For the indirect technique to work, the motor-driver controller must be suitable. This is because the controller also needs to be aware of a few rotor parameters, which may change continuously depending on the operating conditions (Bose, 2002), (M. H. Rashid, 2010).

3. Methodology

The application of the space vector pulse width technique for the switching of the inverter is used with consideration of efficient use of the DC voltage and fewer harmonics distortion to perform the indirect field-oriented control of the induction motor. The implementation of the closed control system for the speed control requires necessary steps and sequences to be followed such as determining the rotor position to ensure that the vector is correctly aligned. The decoupling of the components is possible given the rotor position added with the slip angle. The rotor flux and torque generating current components of stator current must be decoupled suitably respective to the rotor flux vector like separately excited DC motor to obtain necessary torque and speed so that the independent control of the flux and torque is possible and control characteristics are made linear. By incorporating the PI control system and using the Space vector modulation technique, the decoupled control system is used to perform in both transient and steady-state conditions. To convert the time domain components of a three-phase system (in abc frame) to two components in an orthogonal rotating reference frame i.e., components in the $\alpha\beta$ frame to dq frame, Clarke and Park transformation is used in the design. Consecutively implementing these two transforms simplifies computation by converting AC and voltage waveforms into DC signals. To reduce the error in the feedback system, the PI is tuned to obtain the set of gains ensuring the optimum performance of the control system. For components like, torque and speed different PI controllers are added to the system.

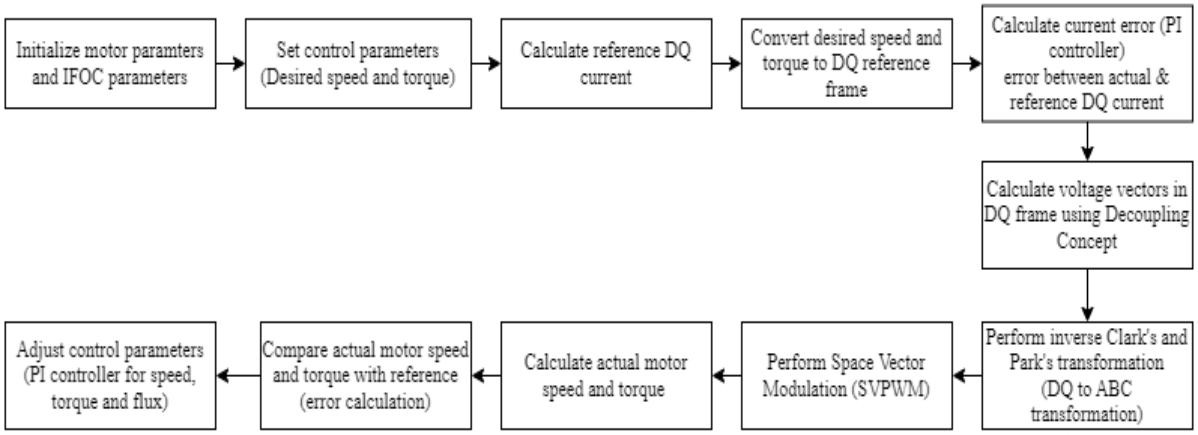

Figure 4. Flow diagram.

3.1 *MATLAB Simulink model for overall system*

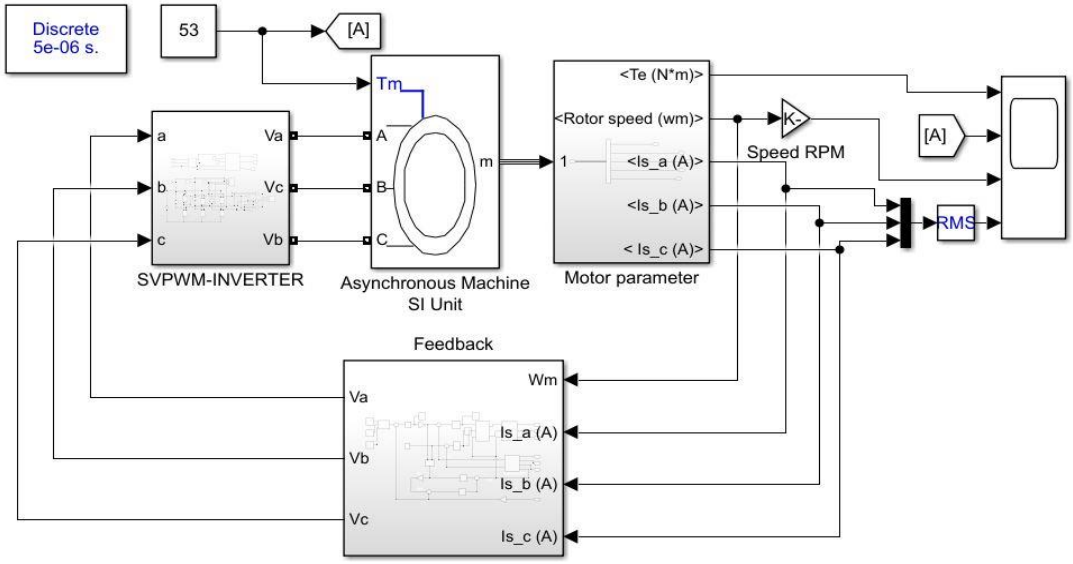

Figure 5. Overall system.

Figure 5 shows the Simulink model of the overall system. The current of each phase and the speed of the Induction motor are taken as feedback which produces voltage signals for the inverter. The inverter produces the required voltage to drive the induction motor at the speed we desire. The feedback includes PI-controller which helps to reduce error and run the induction motor at the reference speed we provide.

3.2 *MATLAB Simulink model for abc to dq stationary transformation*

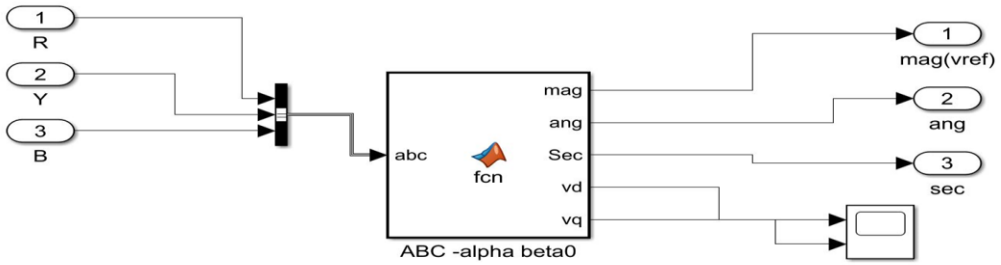

Figure 6. abc to dq stationary transformation.

3.3 *MATLAB Simulink model for SVPWM generation*

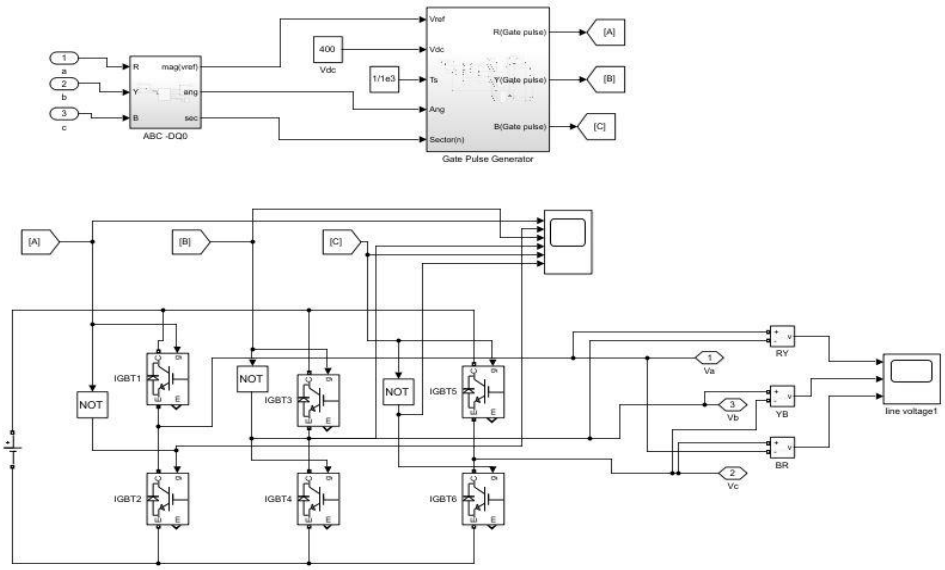

Figure 7. Implementation of SVPWM in MATLAB Simulink

Figure 7 shows the Simulink model for the generation of SVPWM. Here, the functions for obtaining the pulse are done in two different blocks. In the ABC-DQ0 block, the 3- 3-phase ABC voltages are converted to the 2-phase dq voltage and the reference voltage, and the angles are calculated in the same block. From the angle obtained, the sectors are defined from 1 to 6. This reference voltage, angle, DC voltage, and sampling time are fed to the gate pulse generator pulse for determining the switching times. As per the sector and switching time obtained, the switching states are selected to generate gate pulses. The obtained gate pulses are to feed to three-phase inverters.

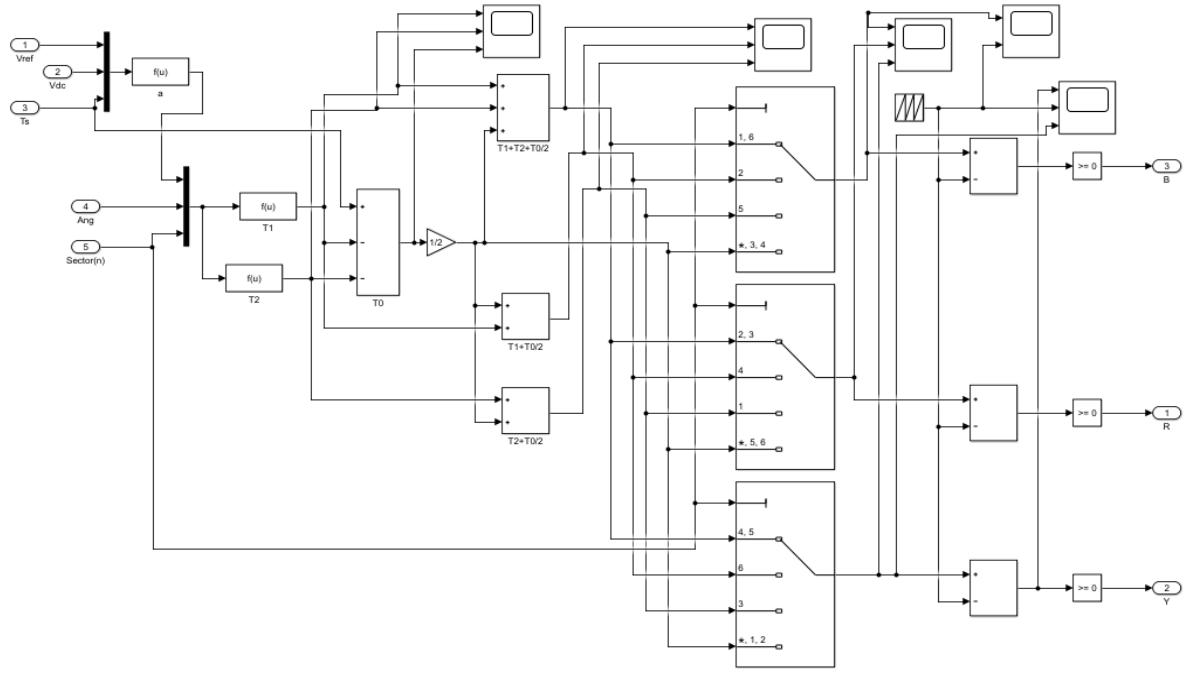

Figure 8. Gate pulse generator

Figure 8 shows the gate pulse generator Simulink model that determines the switching time and sector for generating the PWM pulse.

3.4 *MATLAB Simulink model for IFOC control*

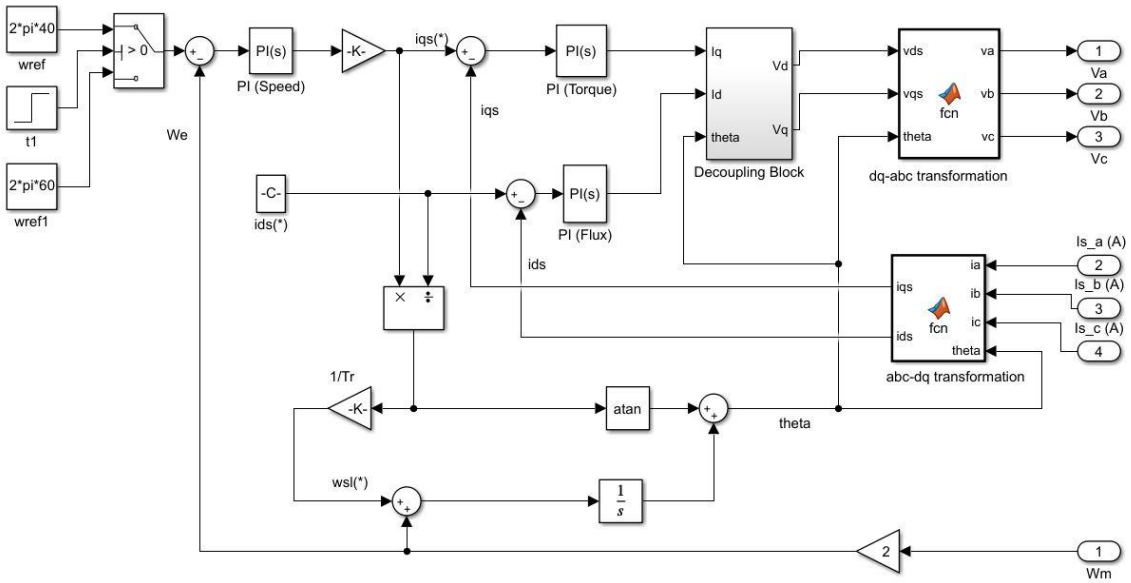

Figure 9. Closed loop control system of the Indirect field-oriented control

Figure 9 shows the closed-loop control using IFOC for controlling the Induction motor. The 3-phase stator current obtained from the Induction motor is converted to the 2- 2-phase I_{ds} and I_{qs} through Clark and Park's transformation. The error signal is fed to the PI controller, which is the speed component; the I^*_{qs} generated is compared with the I_{qs} current from the abc-dq0 transformation block to obtain the error signal and fed it to the PI controller, which is the torque component. Similarly, I^*_{ds} is kept constant that is compared to I_{ds} to obtain the error signal that is fed to the PI controller, which is the flux component. Here, the theta (θ) is the required angle for the decoupling of torque and flux. This angle helps in adjusting the rotor axis frame to the reference rotating frame. It is calculated by taking slip frequency and motor frequency into account.

3.5 *MATLAB Simulink model for decoupling*

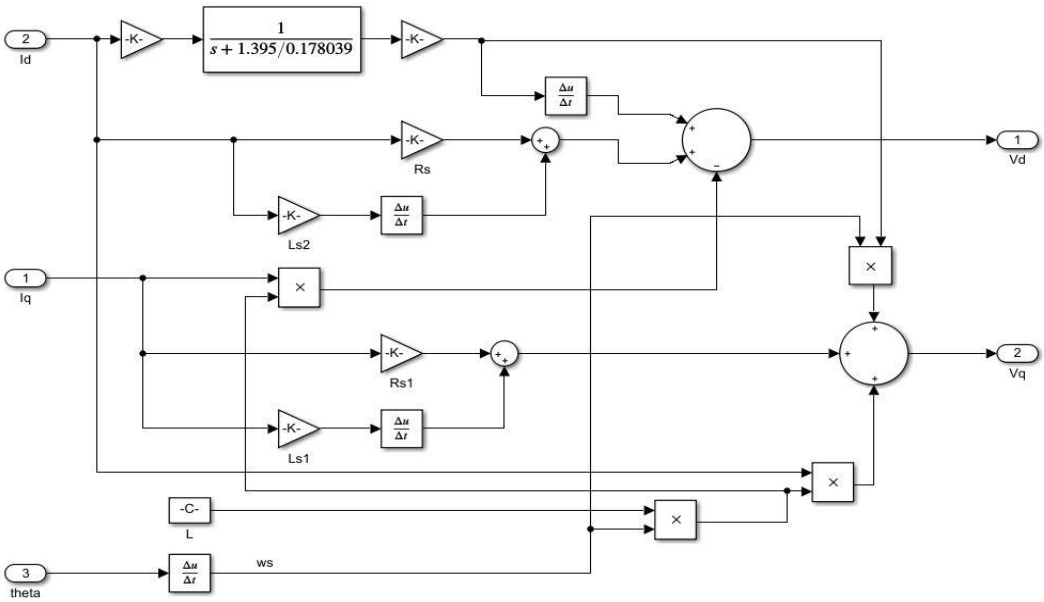

Figure 10. Decoupling block.

A decoupling block decouples the two components of stator current, hence the independent control of the flux and torque is possible and control characteristics are linearized. The dq voltage signal obtained by decoupling is park transformed and the 3-phase ABC voltage signal is obtained that is fed to the SVPWM inverter.

4. Results and Discussion

4.1 *Simulation result for the reference speed of 1200 rpm with constant load torque as 10 Nm.*

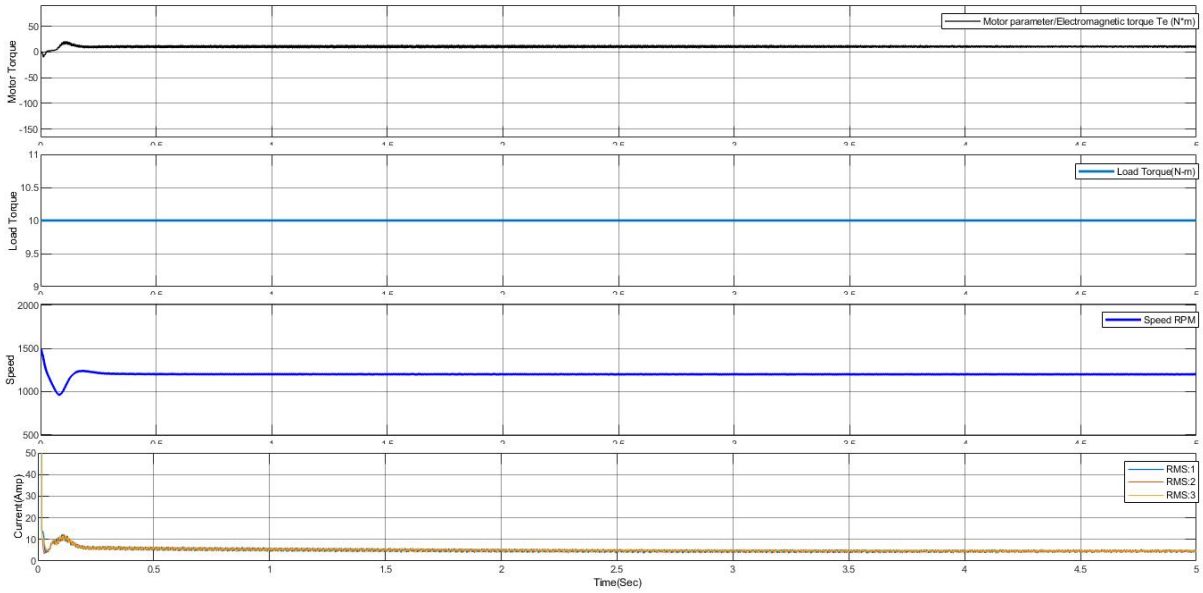

Figure 11. The output waveform of electromagnetic torque, load torque, speed, and stator current with respect to time for 12000 rpm.

4.2 *Simulation result for the reference speed of 1500 rpm with constant load torque as 20 Nm.*

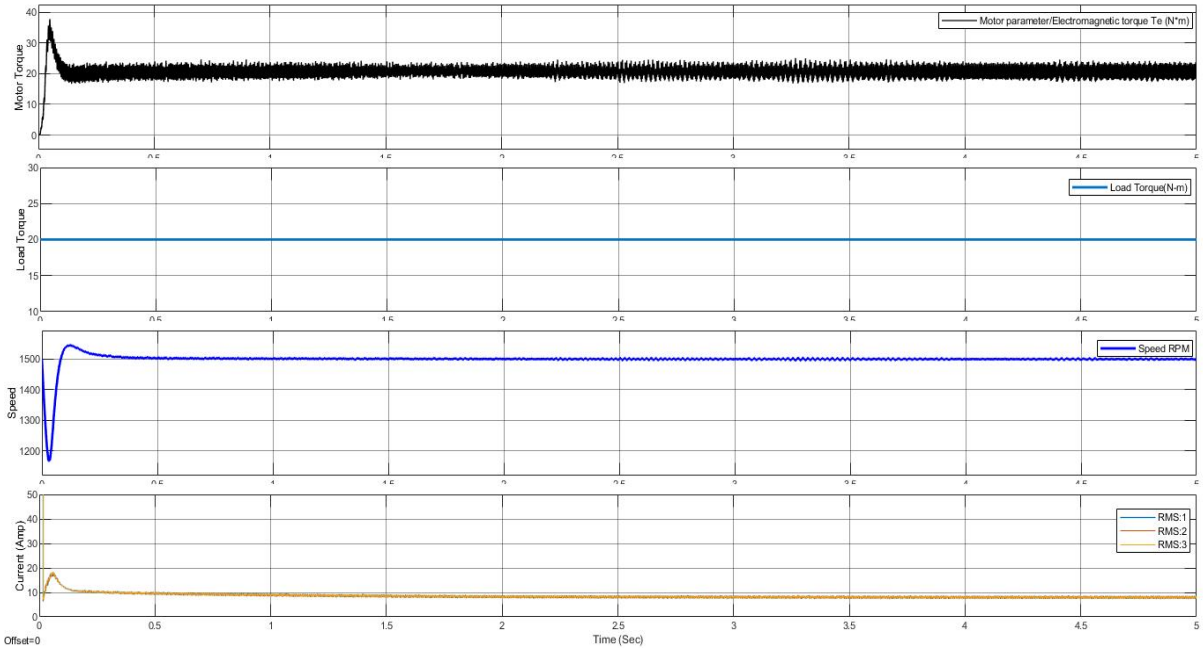

Figure 12. Output waveform of electromagnetic torque, load torque, speed, and stator current with respect to time for 1500 rpm.

4.3 *Simulation result for the reference speed of 1800 rpm with constant load torque as 22 Nm.*

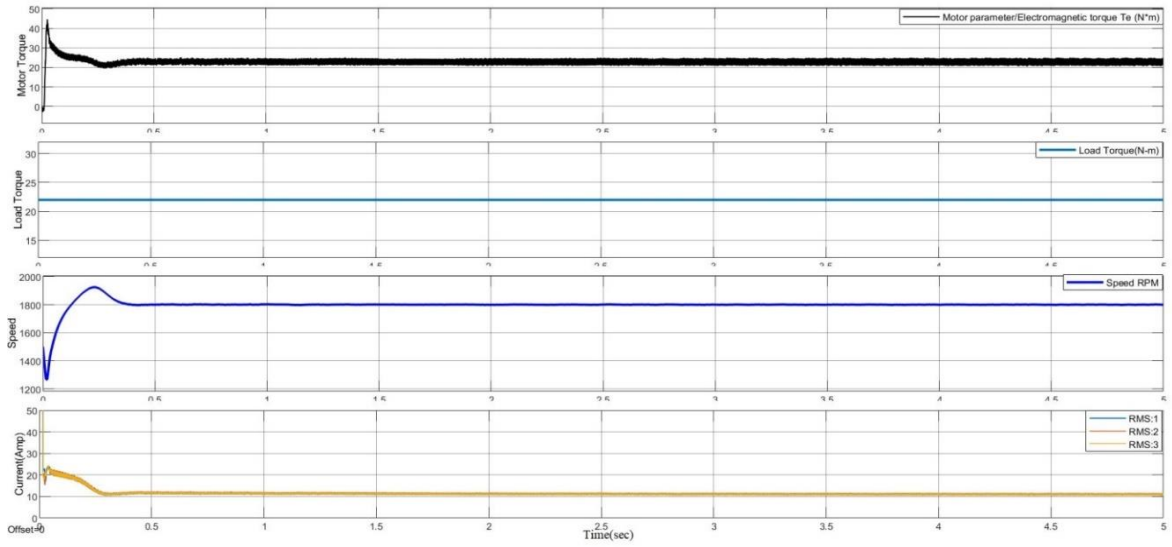

Figure 13. The output waveform of electromagnetic torque, load torque, speed, and stator current with respect to time for 1800 rpm.

Table 3. Discussion of figure 11, 12 and 13

Speed(rpm)	Time(sec)	Torque (Nm)	Starting time to gain reference speed(ms)
1200	up to 5	10	313.47
1500	up to 5	20	364.82
1800	up to 5	22	337.31

From table 3, At time up to 5 seconds when the load torque is 10Nm with a reference speed of 1200rpm, the starting time to gain reference speed was found to be 313.47ms. On increasing load torque to 20Nm with a reference speed of 1500rpm, the starting time to gain reference speed was found to be 364.82ms. Similarly, on further increasing load torque to 22Nm with a reference speed of 1800rpm, the starting time to gain reference speed was found to be 337.31ms. When we apply a constant load torque, the reference speed is maintained after a few milli-seconds as shown in Figures 11, 12, and 13.

4.4 *Simulation result for the reference speed of 1800 rpm by varying the load torque as 15 Nm for 0.75 sec, 10 Nm for 0.75 sec, 5 Nm for 0.75 sec, and 0 Nm for 0.75 sec respectively.*

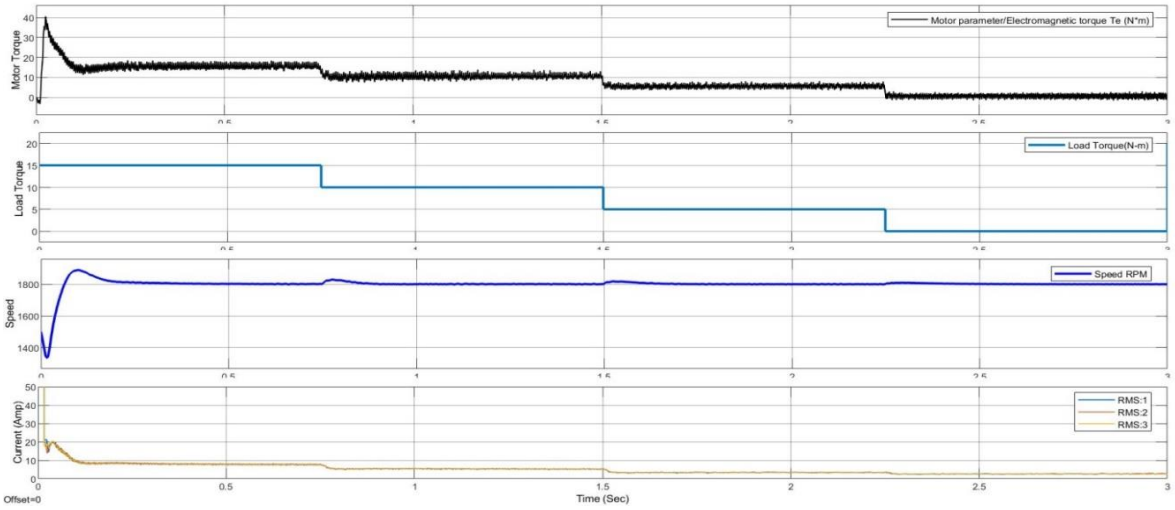

Figure 14. The output waveform of electromagnetic torque, load torque, speed, and stator current with respect to time for 1800 rpm at decreasing step load.

Table 4. Discussion of Figure 14

Speed (rpm)	Time (sec)	Torque (Nm)	Speed recovery time (ms)
1800	0.75	15	112.284
1800	0.75-1.5	10	115.163
1800	1.5-2.25	5	89.25
1800	2.25-3	0	-

From table 4, when the load torque of 15Nm is given for 0.75 seconds the recovery time for speed was found to be 112.284ms. On decreasing load torque from 15Nm to 10Nm in 0.75 to 1.5 seconds the recovery time for speed was found to be 115.163ms. Similarly, on further decreasing load torque from 10Nm to 5Nm in 1.5 seconds to 2.25 seconds the recovery time for speed was found to be 89.25ms. When there is a change in load torque the reference speed is maintained after a few milli-seconds as shown in Figure 14.

4.5 *Simulation result for the reference speed of 1800 rpm by varying the load torque as 0 Nm for 1 sec,5 Nm for 1 sec and 10 Nm for 1 sec 15 Nm for 1 sec, and 20 Nm for 1 sec respectively Such that current increase when the load torque increase.*

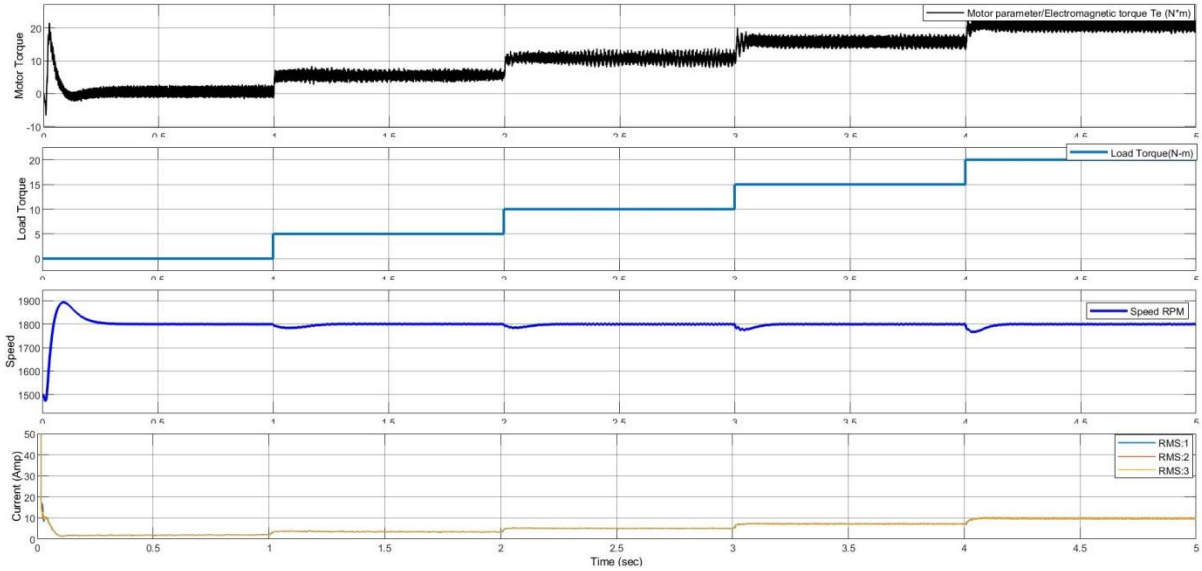

Figure 15. The output waveform of electromagnetic torque, load torque, speed, and stator current with respect to time for 1800 rpm at increasing step load.

Table 5. Discussion of Figure 15

Speed (rpm)	Time (sec)	Torque (Nm)	Speed recovery time (ms)
1800	up to 1	0	-
1800	1-2	5	201.536
1800	2-3	10	167.946
1800	3-4	15	124.76
1800	4-5	20	139.155

From table 5, when the load torque is increased from 0 to 5Nm in 1 to 2 seconds the recovery time for speed was found to be 201.536ms. On increasing load torque from 5Nm to 10Nm in 2 to 3 seconds the recovery time for speed was found to be 167.946ms. Similarly on increasing load torque from 10Nm to 15Nm in 3 to 4 seconds the recovery time for speed was found to be 124.76ms. Before applying 20Nm torque the speed recovery time was found to be decreasing and after applying torque of 20Nm it was found to be increasing and the time was increased to 139.155ms. Now, for the balance condition, the motor torque also increases such that

the stator current increases. When there is a change in load torque the reference speed is maintained after a few milli-seconds as shown in Figure 15.

5. Conclusions

The IFOC is utilized for the control of rotor speed and torque of the induction motor by incorporating the SVPWM technique in this journal. The results of the simulation are used to illustrate the proposed control mechanisms. The speed control of the induction motor using IFOC is achieved by applying three different PI controllers in both transient and steady-state conditions. Results of the IFOC approach were obtained using MATLAB Simulink. Furthermore, the output of the simulation is displayed as motor torque, load torque, speed, and stator current. Five different simulation results are shown with different conditions of load torque and speed. Even varying the load torque at any instant, the desired speed is maintained in a few milliseconds. The synchronous speed of the motor being 1500RPM can be run at a lower speed of 900RPM and a higher speed of 1800 RPM which inherits similar properties of separated excited DC motors.
Further investigation on this paper can be done by tuning PI which can give a higher range of speed if done with precision. This paper describes the maximum threshold speed up to 2340 RPM.

References

Bose, B. K., 2002. *Modern Power Electronics and AC Drives Prentice Hall.* s.l.:Inc, Publication.

BT, V. G., 2017. Comparison Between Direct and Indirect Field Oriented Control of Induction Motor. *International Journal of Engineering Trends and Technology (IJETT),* Volume 43, pp. 364-369.

Hiware, R. S. & Chaudhari, J., 2011. *Indirect field oriented control for induction motor.* s.l., IEEE.

Jung & Jin-Woo, 2005. PROJECT# 2 Space vector PWM inverter. *Mechatronic Systems Laboratory, Dept. of Electrical and Computer Eng. The Ohio State University.*

Kumar, R., Gupta, R. & Bhangale, S., 2007. Indirect vector controlled induction motor drive with fuzzy logic based intelligent controller.

M. H. Rashid, 2010. *Power electronics devices, circuits and applications.* fourth ed. s.l.:Pearson.

Mishra, A., Save, S. & Sen, R., 2014. Space vector pulse width modulation. *International Journal of Scientific & Engineering Research,* Volume 5(2), pp. 1472-1476.

Sirisha, D., n.d. *Comparison of SPWM and SVPWM techniques for vector controlled Induction Motor drive,* s.l.: s.n.

Tiwa & Shashank, 2017. Space vector pulse width modu. *Research Journal of Engineering Sciences,* Volume 6(8), pp. 8-12.